ANNEALING TO MITIGATE PITTING IN ELECTROPOLISHED NIOBIUM COUPONS AND SRF CAVITIES

L. D. Cooley, E. Hahn, D. Hicks, A. Romanenko, R. Schuessler, and C. Thompson

Fermi National Accelerator Laboratory
PO Box 500, Batavia, IL, 60510, U.S.A.

ABSTRACT

Ongoing studies at Fermilab investigate whether dislocations and other factors instigate pitting during cavity electropolishing (EP), despite careful processing controls and the inherent leveling mechanism of EP itself. Here, cold-worked niobium coupons, which exhibited increased tendencies for pitting in our past study, were annealed in a high vacuum furnace and subsequently processed by EP. Laser confocal scanning microscopy and special defect counting algorithms were used to assess the population of pits formed. Hardness measurements indicated that annealing for 2 hours at 800 °C produced recovery, whereas annealing for 12 hours at 600 °C did not, as is consistent with known changes for cavities annealed in a similar way. The 800 °C anneal was effective in some cases but not others, and we discuss reasons why tendencies for pitting remain. We discuss implications for cavities and continued work to understand pitting.

KEYWORDS: SRF cavities, niobium, electropolishing, electron-beam weld, pits.

INTRODUCTION

Pits associated with the heat-affected zone (HAZ) of equatorial welds on superconducting radio-frequency (SRF) cavities continue to pose limitations on the achievement of high accelerating gradient [1]. Pits are observed on about 3% of cavity equator electron-beam welds [2], and even though some are (curiously) benign, roughly one cavity in every five is limited by quench at a pit location. Since the collision energy of a linear accelerator composed of SRF cavities is determined by the average accelerating gradient per cavity, developing strategies to reduce tendencies for pit formation, or prevent them from forming altogether, has a direct benefit for high-energy physics.

Several possible origins of pits have been discussed, based largely on analyses of the fabrication and processing procedures and of the images of pits acquired by special optical inspection systems developed for SRF cavities [3]. Bubbles of trapped gas might occur when small defects are vaporized by the electron beam [1], or possibly when hydrogen incorporated during pre-weld etching becomes accumulated. Such bubbles would be consistent with the spherical shape noted for many pits [4]. Interstitial contaminants also diffuse along the thermal gradient and accumulate at the HAZ boundary, as indicated by resistivity measurements [5]. Such pockets might lead to local stress and high material removal rate, which could occasionally result in the formation of a pit with faceted edges, as is also observed. Likewise, dislocations can be concentrated at the HAZ border [6], making those regions susceptible to dislocation-assisted pitting, as is well known for niobium [7, 8]. It should be noted that cavity equatorial welds are not stress relieved, and that cold work is not removed from pieces prior to pre-weld acid etching or welding. We focus on this third possibility in the present article.

Chemical polishing of niobium requires both the conversion of niobium metal to its oxide and the subsequent dissolution of the niobium oxide via conversion to a fluoride or chloride. Dislocations permit deep penetration of oxygen and fluorine, as well as attack along crystallographic directions other than those which are normal to the local surface. Deep pits can thus result [7, 8]. Indeed, in our past study of niobium coupons [9], significantly higher tendency for pitting was observed for cold-worked coupons than for recrystallized coupons. Electropolishing has been used to circumvent deep material removal by establishing a fluorine ion gradient near the niobium surface [10]. This has been very successfully applied to SRF cavities [11], with excellent results following from carefully controlled production processes using custom built equipment at many locations worldwide. EP is the preferred technique of polishing SRF cavities at present [12].

However, occasionally the EP process can go wrong. Recent work [13] showed that the fluorine ion gradient may be disturbed by circulation of the electrolyte, especially at high temperature (e.g. 45 °C instead of 30 °C) where the viscosity is low. The disturbances evidently supply fluorine ions to the low points of the niobium surface, thereby permitting attack in addition to the diffusion-limited leveling intended by EP. In our past study [9], deliberate agitation of the electrolyte produced surface finishes akin to those made by simple etching. Thus, it is plausible that an EP process can on occasion produce flaws such as dislocation-assisted pitting. This was the main result of our past study [9]—Cold work makes SRF cavity niobium susceptible to flaws when the EP process deviates from its baseline settings. The next logical question is whether annealing to remove cold work prior to etching should improve the resiliency of the niobium metal against EP process flaws. This is the work reported here.

EXPERIMENT

The same niobium coupons as processed in our previous study [9] were used in the present work. In brief, coupons were cut from cavity-grade niobium sheets. Some were kept in the 95% recrystallized as-received state, referred to as “AR”. Other coupons, referred to as “CW”, were cross-rolled to simulate the cold work applied to half cells during forming. A total reduction of thickness by 40% was applied. Some AR and CW coupons were subsequently welded by various vendors who produce SRF cavities, using the same machines and preparation as for cavities. EP was subsequently applied using an apparatus specifically built to mimic the flow, temperature, voltage, and other conditions of cavity EP [9]. Various features were then noted, such as gloss, roughness, and pits.

In the present experiment, the CW coupons were annealed in a Thermacraft 1200°C high, vertical vacuum furnace specifically designed to remove interstitial impurities from niobium. A 2,000 L/s turbo-molecular pump backed by a 500 L/s Anesta Iwata scroll pump produced vacuum better than 10^{-6} torr at maximum temperature (base < 10^{-8} torr). The design of the pumps was chosen for efficiency at removing hydrogen and oxygen and for their compression ratio. Heat treatments were carried out with a soak of either 12 hours at 600 °C (referred to as A6 coupons) or 2 hours at 800 °C (referred to as A8 coupons), with a ramp up rate no higher than 5 °C/min and furnace cooling over approximately 18-20 hours after the soak. Vacuum was kept until the parts were below 70 °C, followed by venting with dry nitrogen and promptly sealing the coupons in bags with a nitrogen purge.

Images of the coupon surface were acquired by scanning on a flat bed scanner and by stitching together images from a laser confocal scanning microscope (LCSM, Keyence model VK-9700). After annealing, the coupons surfaces were "reset" by mild sand blasting with 50 µm diameter alumina sand, followed by a short etching to remove any grit along with 20 µm of material. This etching revealed grain contrast near the welds, which allowed the HAZ to be located. An image was acquired, and comparison of this image with that taken at the end of the previous study was used to assess any changes in grain structure that might have occurred during annealing. Subsequently, a deep EP process was applied to remove approximately 100 µm of metal. The EP was carried out as before [9], at 30 °C, 14.5 V, 500 A m^{-2}, with a 1:20 area ratio of Al cathode to Nb coupon anode, and with sufficient circulation of the electrolyte to completely exchange the volume once per minute (as is true of a SRF cavity EP process). A second image was acquired after EP.

The LCSM provides the capability to count defects over large areas via image stitching and special algorithms. Since a confocal microscope uses a pinhole to eliminate out-of-focus light from a certain focal plane, objects above or below the focal plane can be rejected from an image. If the in-focus light is then cast as a single color (e.g. black) and combined with the rejected objects (colored e.g. white), a binary image can be composed. This technique was applied to create binary images with resolution determined by the pixel dimensions (approximately 10 µm at the settings used). Objects with area greater than 100 and 400 pixels in area were counted. Scratches and other large defects were filtered from the binary images by the operator setting an arbitrary level, e.g. 100 pixels in one dimension or 1000 pixels in area, for objects to be ignored. As will be discussed, merged objects were difficult to analyze objectively. We did not re-touch any images to try to separate objects for analysis. In addition, coupons polished during our earlier work were re-analyzed by the LCSM to provide consistency. Pit counts are based a scanned area of 1 cm x 1 cm. Three different areas on each sample were scanned and then the average value noted in the spreadsheet.

Hardness was measured to assess the degree to which heat treatments recovered cold work. Since the metals were soft, hardness was determined using a 3.2 mm spherical steel ball indenter with 60 kg equivalent force. Hardness values reported here refer to the Rockwell H scale. For example, AR coupons registered hardness of ~75 HRH, which roughly converts to ~60 Vicker's hardness as stipulated by specification [14].

RESULTS

Figure 1 shows example images of A6 and A8 coupons obtained from a flat-bed scanner. The lower images were acquired after sand blasting and light etching. The HAZ

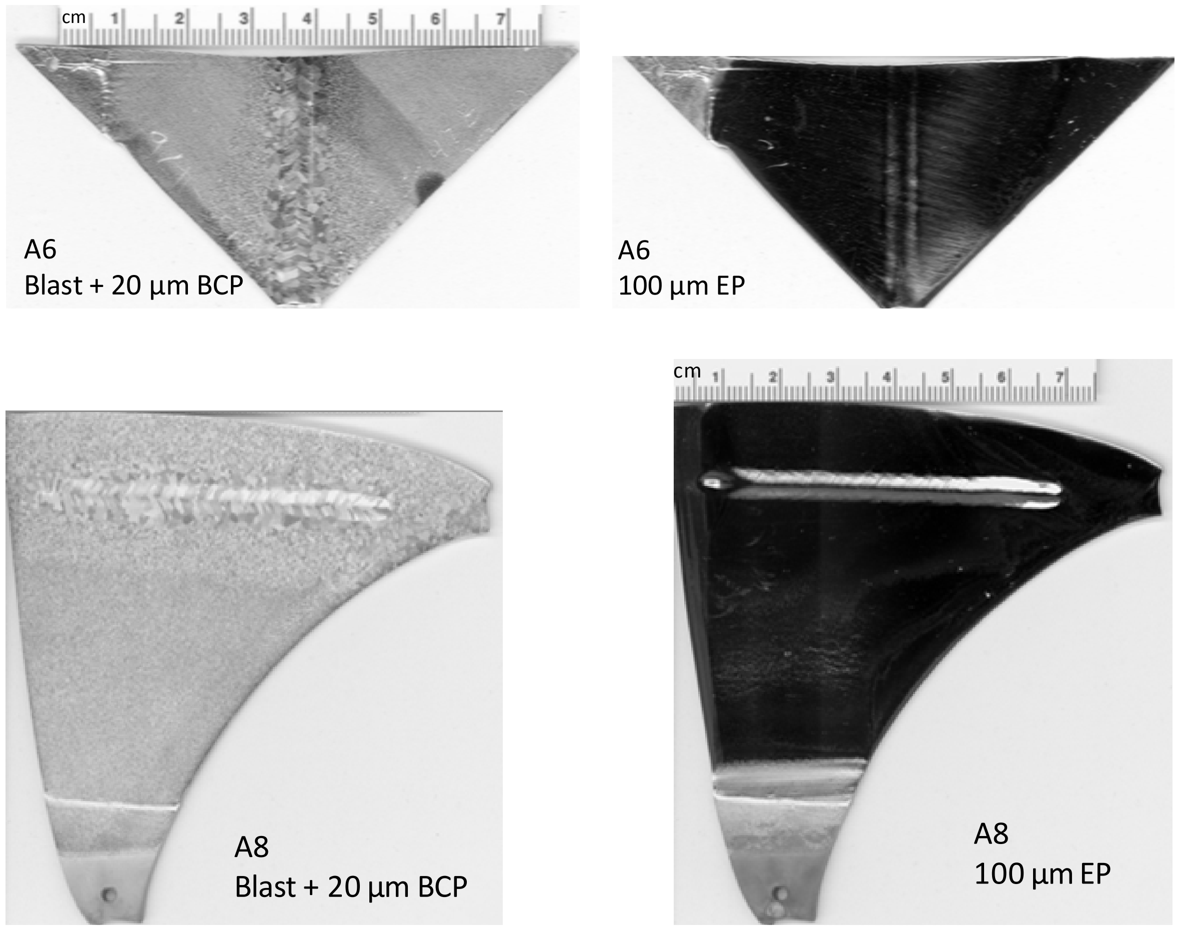

FIGURE 1. Images of example A6 (top) and A8 (bottom) coupons after sand blasting plus 20 µm etch (left), and after EP (right). BCP refers to “buffered chemical polishing”. The dark color of the right images is an artifact of the high coupon gloss when acquired by a flat-bed scanner.

is clearly evident, and large defects were effectively removed by the “resetting” treatment. The upper images were acquired after 100 µm of metal was removed by EP. Gross defects are not seen. As noted in the previous study, the high gloss of the EP surfaces produces dark images due to the angle between illumination source and photodetector.

Figure 2 shows hardness data for the AR and CW coupons. The softening of the metal near the weld is clearly evident, as is the extent of the HAZ. The plateau regions indicate the base hardness of the coupon itself. This is 75 ± 3 HRH for the AR coupons and 95 ± 4 HRH for the CW coupons. The lack of data points for the AR coupons between 5 and 10 mm distance from the weld is due to the location of an edge machined into the coupon to re-create the weld preparation of the cavity cell [9]. It was not possible to properly support the coupon on the hardness tester anvil for these locations. Figure 2 also shows the hardness data for the A6 and A8 coupons. The A6 coupons show hardly any reduction in hardness compared to the CW coupons. By comparison, the A8 coupons show a return to the 75 HRH hardness of the AR coupons. It can be concluded that the 800 °C anneal produced recovery, whereas the A6 anneal did not.

Examples of the binary images, from which areas were sampled for pit counting, are shown in Figure 3. It is interesting to note that some defects have chevron shape, as would be characteristic for dislocation-assisted pitting [7]. This was not revealed by our earlier study due to lack of sufficient resolution by the image analysis technique.

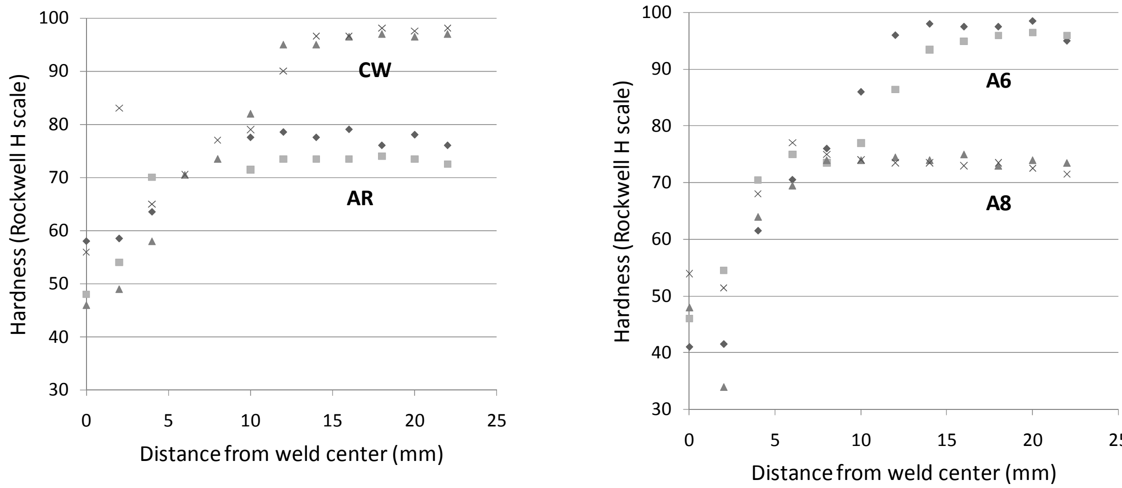

FIGURE 2. Hardness data for the coupons before (left plot) and after (right plot) annealing.

Table 1 presents pit populations normalized to 2 cm x 2 cm area for the range of coupons discussed. While there is significant scatter in the data, trends from our previous study are evident. Namely, (a) AR coupons have low populations of pits; (b) many CW coupons have high populations of pits; about 5-8 times that of AR coupons; and (c) welds tend to increase pit counts. The data for the A6 coupons lie in the same range **as f**or the CW coupons, with somewhat higher counts of big pits compared to smaller pits. Perhaps some coarsening of pits has been instigated by the 600 °C anneal. The A8 coupons exhibit pit populations between those of AR and CW coupons, suggesting an intermediate population. As for the A6 coupons, the count of large pits is proportionately higher.

DISCUSSION

The assessment of defects in coupons is somewhat arbitrary and subject to the level of scrutiny by the operator. Here, we have attempted to remove human factors as much as possible to obtain an objective count of defects as a function of the coupon material and its processing via the LCSM. Scatter in the data is indicative both of real variations among the sample examined as well as image acquisition conditions such as glossiness, drift,

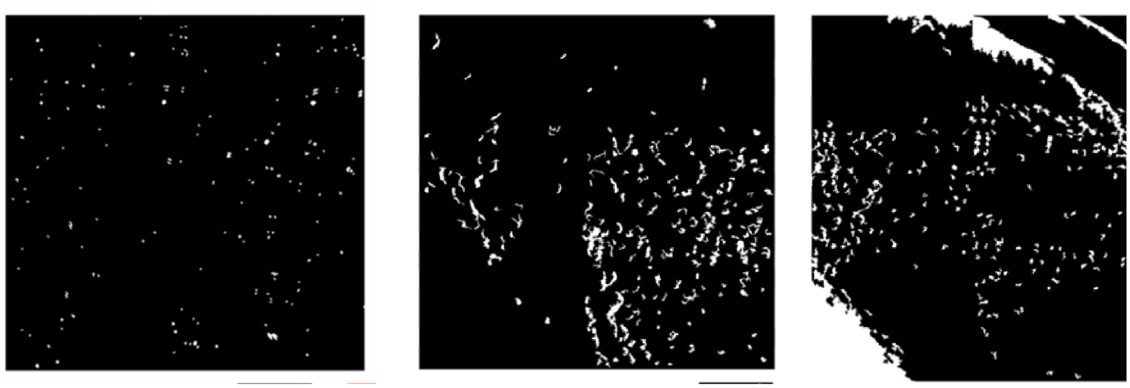

FIGURE 3. Example binary images used for pit counting. At left is a 2 cm x 2 cm scan of a CW coupon. At center is a 1 cm x 1 cm scan of an A6 coupon. At right is a 1 cm x 1 cm scan of an A8 coupon. The weld and corresponding HAZ run diagonally across the lower left corners of the center and right images.

TABLE 1. Results of pit populations for different coupon series after EP.

Coupon Series	Number	Pits > 100 μm	Pits > 200 μm
AR	EP-6	5	0
	EP-10	1	0
	EP-12	1	0
AR + weld	WS-27	17	1
	WS-30	1	0
CW			
	CW-2	39	3
	CW-4	10	1
	CW-6	39	2
CW + weld	WAC-34	36	2
	WSC-P2	12	1
A6 CW + weld	WSC-47B	6 to 200 (objects merge)	
A8 CW + weld	WSC-P4	7	2
	WAC-36A	20	1
	WSC-47A	30	2

vibration, and other instrument errors. However, the images in Figure 3 clearly show that the binary objects occur in clusters and can tend to overlap. The data then become rather sensitive, for some coupons, to the particular area of the scan and the level used to cut off large objects. Since we did not touch up any images to attempt to separate objects, multiple scans were used to try to average out the clustering effects. This did not work for the A6 samples, because the merging of objects made the data for any scan sensitive to different cut-off levels.

The main trends from our previous study are supported by the LCSM pit counts on those repeated samples. AR samples have very low pit counts (7 coupons were analyzed), whereas CW coupons have markedly elevated pit counts. Welding also seems to exacerbate pitting somewhat. Inserted, now, are the additional data for A6 and A8 coupons. Some reduction of pit counts is found in two of the three A8 samples, as compared with the CW samples. However, the binary image in Figure 3 and the one coupon with high pit count in Table 1 indicate that improved pitting behavior is not always achieved. More work is needed to add coupons to the Table 1 list.

The chevron shapes of the pits, as exemplified in Figure 3, after annealing is curious. This is the shape expected for dislocation-assisted pitting [7,8]. Why it is absent in the CW samples could indicate that the dislocations are effectively dispersed in the CW samples, whereas they are clustered in the A6 and A8 samples. Since 800 °C is not sufficient to begin recrystallization, the net effect of the annealing may be to cluster dislocations into geometric bands, thereby concentrating them in certain regions [15]. The concentrated dislocation bands might actually make the metal more susceptible to pitting, not less. It is interesting that the A8 samples show some large pits as well.

An uncontrolled factor in the experiment is the use of buffered chemical polishing (BCP). Since all welded samples require an etch of ~ 20 μm to produce clean surfaces, and this etch is commonly done by BCP, it may be possible that the pits are actually artifacts of the BCP instead of being created during the EP as we supposed. The rough surface after

BCP makes identifying and counting pits practically impossible to test whether BCP produces copious pitting that EP cannot remove. Moreover, since it was necessary to remove any pits from the CW samples to assess the effects of annealing, the sand-blast and BCP may have re-conditioned the A6 and A8 samples with similar artifacts. Changes in etching procedure, such as using diluted BCP, could be used to test this hypothesis.

CONCLUSIONS

Annealing niobium coupons that were previously cold-worked at 800 °C for 2 hours produced recovery of cold work, which was accompanied in some samples by a reduction of the population of pits created during EP. However, some binary images and one sample did not indicate any reduction in pitting tendency. In no case did annealing reduce pit counts to a level found for as-received sheets in a 95% recrystallized state. Data for coupons annealed at 600 °C were difficult to analyze due to merging of the image objects. In both sets of annealed coupons, chevron shapes and some coarsening of the pits were observed, which merits further investigation to understand whether coalescence of dislocations during recovery sets up increased dislocation-assisted pitting. This is important because larger pits tend to have more adverse of an effect on SRF cavities.

ACKNOWLEDGEMENTS

Fermilab is operated by Fermi Research Alliance, LLC under Contract No. DE-AC02-07CH11359 with the United States Department of Energy. We thank W. Starch for technical assistance with rolling the coupons. Assistance by M. Foley, J. Rathke, and R. Edinger is also acknowledged. Discussions with C. Cooper, A. Rowe, M. Champion, C. Reece, A. Dzyuba, C. Ginsburg, and D. Sergatskov are also acknowledged.

REFERENCES

1. M. S, Champion, L. D. Cooley, C. M. Ginsburg, D. A. Sergatskov, R. L.Geng, H. Hayano, Y. Iwashita, and Y. Tajima, “Quench-limited SRF cavities: Failure at the heat-affected zone”, *IEEE Trans. Appl. Supercond.* **19**, pp. 1384-1386 (2009).
2. D. A. Sergatskov and E. Toropov, Fermilab, private communications.
3. Y. Iwashita, Y. Tajima, and H. Hayano, “Development of high resolution camera for observations of superconducting cavities”, *Phys. Rev. ST Accel. Beams* **11**, 093501 (6 pp), (2008).
4. K. Watanabe, “Review of optical inspection methods and results”, Proc. SRF 2009 (electronic), Berlin, Germany, 2009, p. 123, https://accelconf.web.cern.ch/accelconf/SRF2009/papers/tuobau01.pdf .
5. S. Anakhov, X. Singer, W. Singer, and H. Wen, “Gas and RRR distribution in high purity niobium EB welded in ultra-high vacuum”, AIP Conf. Proc., vol 837, pp 71-84 (2006).
6. T. R. Bieler *et al.*, “Physical and mechanical metallurgy of high purity Nb for accelerator cavities”, *Phys. Rev. ST Accel. Beams* **13**, 031002 (13 pp), (2010).
7. X. Zhao, G. Ciovati, C. E. Reece, and A. T. Wu, “Surface topography of “hotspot” regions from a single cell SRF cavity”, Proc. PAC09 (electronic), Vancouver BC, (2009) http://trshare.triumf.ca/~pac09proc/Proceedings/papers/we5pfp062.pdf.
8. P.R. Evans, “Dislocation Etch Pit Studies in Annealed and Deformed Polycrystalline Nb”, *J. Less Common Metals* **6**, pp. 253-265 (1964).
9. L. D. Cooley, D. Burk, C. Cooper, N. Dhanaraj, M. Foley, D. Ford, K. Gould, D. Hicks, R. Novitski, A. Romanenko, R. Schuessler, C. Thompson, and G. Wu, “Impact of Forming, Welding, and Electropolishing on Pitting and the Surface Finish of SRF Cavity Niobium”, *IEEE Trans. Appl. Supercond.* **21**, 2609-2614 (2011).

10. H. Diepers, O. Schmidt, H. Martens, and F. S. Sun, “A new method of electropolishing niobium”, *Physics Lett. A* **37**, pp 139-140 (1971).
11. K. Saito, H. Inoue, E. Kako, T. Fujino, S. Noguchi, M. Ono, and T. Shishido, “Superiority of electropolishing over chemical polishing on high gradients”, Proc. 1997 Wkshp. RF Supercond., Padova, Italy (electronic), http://accelconf.web.cern.ch/AccelConf/SRF97/papers/srf97d02.pdf.
12. TESLA Technology Collaboration, “Final surface preparation for superconducting cavities”, TTC-Report 2008-05, available at http://flash.desy.de/reports_publications/tesla_reports/tesla_reports_2008/ .
13. H. Tian, S.G. Corcoran, C. E. Reece, and M. J. Kelley, “The mechanism of electropolishing of niobium in hydrofluoric-sulfuric acid electrolyte”, *J. Electrochem. Soc.* **155**, pp. D563-D568 (2008).
14. Technical Specification for High RRR Grade Niobium Sheet and Rod for use in Superconducting Cavities, Fermilab specification 5500-ES-371037-A, 2007.
15. T.R. Bieler *et al.*, “Physical and mechanical metallurgy of high purity Nb for accelerator cavities”, *Phys. Rev. ST Accel. Beams* **13**, 031002 (13 pp), (2010).